Off-shore Bidding Zones under Flow-Based Market Coupling

Kenis, Michiel; Delarue, Erik; Bruninx, Kenneth; Dominguez, Fernando

DOI
10.1109/PowerTech55446.2023.10202755

Publication date
2023

Document Version
Final published version

Published in
2023 IEEE Belgrade PowerTech, PowerTech 2023

Off-shore Bidding Zones Under Flow-Based Market Coupling

Michiel Kenis,
Erik Delarue
Applied Mechanics & Energy Conversion
KU Leuven
Leuven, Belgium
{michiel.kenis, erik.delarue}@kuleuven.be

Kenneth Bruninx
Technology, Policy & Management
TU Delft
Delft, The Netherlands
k.bruninx@tudelft.nl

Fernando Dominguez
Energy Technology
VITO/EnergyVille
Genk, Belgium
fernando.dominguez@vito.be

***Abstract*—The market integration of hybrid off-shore projects, consisting of wind farms and transmission assets connecting different market zones, requires re-examining bidding zone definitions. Policy makers consider separate off-shore bidding zones to optimally integrate off-shore wind farms in power systems. In this paper, we apply Advanced Hybrid Coupling to include off-shore DC transmission lines in flow-based market coupling, and compare different bidding zone configurations. We find that off-shore bidding zones lead to a transfer of welfare: the producers' surplus of off-shore wind farm owners decreases as a result of a lower average price and the congestion rent for TSOs increases. Despite that an off-shore bidding zone signals transmission scarcity better, it impacts the need for support instruments for off-shore wind farms.**

***Index Terms*—Advanced Hybrid Coupling, Bidding zone configuration, Flow-Based Market Coupling, Off-shore wind power, Standard Hybrid Coupling**

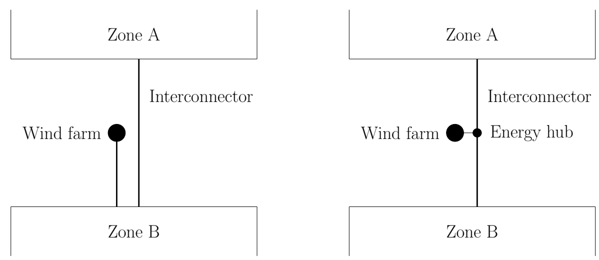

(a) Single-purpose projects (b) Dual-purpose project

Fig. 1: Configuration of off-shore wind farm connection: directly with mainland (single purpose: renewable generation integration or cross-border trade) or via an energy hub (dual purpose: renewable generation capacity and cross-border trade).

I. Introduction

The share of off-shore wind power in the European electricity mix has been increasing and will continue to do so in the future with the European Commission aiming for an installed capacity of 60 GW by 2030 [1]. A large part of these growing wind farms are being developed as part of off-shore energy hubs[1]. In these hubs, the wind farms are connected with an interconnector (generally operated as HVDC lines[2]). Fig. 1 visualises the concept of energy hubs.

In the current market zone configuration, wind farms are part of the mainland zone they are (administratively) connected with, meaning they receive an electricity wholesale price equal to the mainland price. However, this might result in suboptimal price signals and flows [4]. To integrate these new assets (hybrid projects) in the European electricity market, the EU strategy for the deployment of off-shore generation plants opts for an off-shore market zone [5]. It argues that off-shore market zones allow renewable energy to flow where it is needed the most. Besides, the EU claims that it reduces costs from remedial actions and increases operational security because the transmission constraints would be better reflected in the market [4], [6], [7].

However, Transmission System Operators (TSOs) argue that current studies are biased because of two reasons [8]. Firstly, current studies adopt a too simplistic network setup, e.g., by reducing a mainland zone to one node. Secondly, current studies consider a 'Net Transfer Capacities'-methodology to calculate and allocate transmission capacity, while Flow-Based Market Coupling (FBMC) is the preferred methodology in the EU to include transmission constraints in zonal electricity markets.

This paper compares two market zone configurations: one where wind farms are administratively connected to their home market zone, and one where an off-shore market zone is operational. We measure prices, revenues for off-shore wind farms, day-ahead generation and redispatch costs, and congestion rents. We fill the gap in literature by considering FBMC while applying our models on a detailed network (e.g., not aggregating the nodes in a mainland zone to one node). We model the flow-based domains in two ways: (i) by adopting Standard Hybrid Coupling (SHC), and (ii) by adopting Advanced Hybrid Coupling (AHC). The one is the model currently used, and the latter is the target model of the

[1]Examples are the Modular Off-shore Grid of the Belgian TSO Elia and the North Sea Wind Power Hub programme of the German, Dutch and Danish TSOs [2].

[2]Examples are the Nemo link between Belgium and the UK, the Cobra cable between Denmark and The Netherlands, the Celtic interconnector between Ireland and France, the Viking link between the UK and Denmark and the NorthConnect cable between Norway and the UK [3].

2023 IEEE Belgrade PowerTech | 978-1-6654-8778-8/23/$31.00 ©2023 IEEE | DOI: 10.1109/POWERTECH55446.2023.10202755

TSOs to include both AC-lines and DC-lines as well as their interdependence in a market model [9]. We introduce a nodal market clearing as a benchmark because a nodal market design optimally reflects the value of transmission capacity through the prices.

The remainder of this paper is structured as follows. Section II introduces the methodology, Section III presents a case study and Section IV derives policy recommendations and concludes.

II. MODEL

We present two sequential optimisation problems: the day-ahead market clearing using the flow-based methodology and a redispatch problem that takes the outcome of the day-ahead market clearing as parameters. Note that the zone configuration (e.g., an off-shore bidding zone) only affects the set of cross-border transmission lines which serves as an input to the problems. We distinguish two representations of the grid limitations in the market clearing algorithm. Firstly, SHC represents the flow on the AC-lines and DC-lines separately. Specifically, AC-lines are modeled with the flow-based methodology while DC-lines are modeled with an NTC-approach. This is in line with the current approach in reality. Secondly, AHC augments SHC by considering the interdependence between the flow on the AC-lines and DC-lines. This is the target model by TSOs. Finally, we use a nodal market clearing as a benchmark but do not provide the mathematical formulation.

A. Day-ahead market

Equations (1) describe the day-ahead market clearing without grid constraints. Equation (1a) minimises the day-ahead generation cost DAC, which equals the sum over each non-intermittent generator $g \in \mathcal{G}$ of its marginal cost MC_g times its scheduled production $v_g \cdot Q_g^s$ as we assume the cost of production of RES equals zero. Q_g^s is the production capacity of generator g. Equation (1b) limits relative production v_g of each non-intermittent generator g and (1c) limits the curtailment c_n to the injection from RES R_n for each node $n \in \mathcal{N}$. While (1d) presents an intra-zonal power balance for each zone $z \in \mathcal{Z}$ by equaling the net export position p_z to the difference between zonal production and demand, (1e) does the same by equaling the net export position p_z to the flow f_l and f_h^{DC} on each cross-border AC-line l and DC-line h respectively flowing out of zone z. Q_n^d is the load at node n. $I_{l,z}$ and $I_{h,z}$ equal 1 (or -1) when l and h are cross-border AC-lines and DC-lines whose flow is defined outward (or inward) zone z, and is otherwise 0.

$$\min_{v_n, p_z, c_n, f_h^{DC}} \quad DAC = \sum_{g \in \mathcal{G}} MC_g \cdot Q_g^s \cdot v_g \tag{1a}$$

subject to

$$0 \leqslant v_g \leqslant 1, \forall g \in \mathcal{G} \tag{1b}$$

$$0 \leqslant c_n \leqslant R_n, \forall n \in \mathcal{N} \tag{1c}$$

$$\sum_{g \in \mathcal{G}(\mathcal{Z})} Q_g^s \cdot v_g + \sum_{n \in \mathcal{N}(\mathcal{Z})} R_n - c_n - Q_n^d = p_z, \forall z \in \mathcal{Z} \tag{1d}$$

$$\sum_{l \in \mathcal{L}} f_l \cdot I_{l,z} + \sum_{h \in \mathcal{H}} f_h^{DC} \cdot I_{h,z} = p_z, \forall z \in \mathcal{Z} \tag{1e}$$

Equations (1) are common for the two zonal market designs, and are augmented by (2a) to (2c) in case of SHC and by (3a) to (3c) in case of AHC.

1) Standard Hybrid Coupling: Under SHC, the limitations of the AC-lines are represented using the flow-based methodology, while those of the DC-lines fall under the NTC-methodology by definition [9]. This is because the control of the converter between an AC-line and a DC-line allows to control the power flow on the DC-line. Equations (2a) to (2c) present the additional constraints to (1).

$$p_z^{FB} = p_z - \sum_{h \in \mathcal{H}} f_h^{DC} \cdot I_{h,z}, \forall z \in \mathcal{Z} \tag{2a}$$

$$-RAM_l^- \leqslant \sum_{z \in \mathcal{Z}} zPTDF_l^z \cdot p_z^{FB} \leqslant RAM_l^+, \forall l \in \mathcal{L} \tag{2b}$$

$$-NTC_{z,z'}^- \leqslant \sum_{h \in \mathcal{H}} f_h^{DC} \cdot I_{h,z,z'} \leqslant NTC_{z,z'}^+, \forall z, z' \in \mathcal{Z} \tag{2c}$$

Equation (2a) defines the net position p_z^{FB} of each zone z that impacts the flow-based domain. Equation (2b) limits the estimated flow on the critical AC-lines with RAM_l^- and RAM_l^+ in both flow directions. Note that we include all AC-lines as critical AC-lines. The flow is estimated using zonal PTDFs $PTDF_l^z$. Finally, (2c) limits the flow on the cross-border DC-lines between zone z and z' with $NTC_{z,z'}^-$ and $NTC_{z,z'}^+$ in both flow directions. $I_{h,z,z'}$ equals 1 (or -1) in case DC-line h is a cross-border line from zone z to z' (or z' to z), and is otherwise 0. As a consequence, DC-lines that are not cross-border lines are not monitored in the market which is consistent with the NTC-methodology.

2) Advanced Hybrid Coupling: AHC augments SHC by considering the impact of DC-flows on AC-flows. Equations (3a) to (3c) present the additional constraints to (1).

$$p_z^{FB} = p_z - \sum_{h \in \mathcal{H}} f_h^{DC} \cdot I_{h,z}, \forall z \in \mathcal{Z} \tag{3a}$$

$$\begin{aligned} -RAM_l^- \leqslant & \sum_{z \in \mathcal{Z}} zPTDF_l^z \cdot p_z^{FB} \\ & + \sum_{h \in \mathcal{H}'} f_h^{DC} \cdot \big[nPTDF_l^{n(h-)} \cdot I_{n(h-),h}^{ACDC} \\ & + nPTDF_l^{n(-h)} \cdot I_{n(-h),h}^{ACDC} \big] \leqslant RAM_l^+, \forall l \in \mathcal{L} \end{aligned} \tag{3b}$$

$$-NTC_{z,z'}^- \leqslant \sum_{h \in \mathcal{H}} f_h^{DC} \cdot I_{h,z,z'} \leqslant NTC_{z,z'}^+, \forall z, z' \in \mathcal{Z} \tag{3c}$$

Equations (3a) and (3c) are identical to (2a) and (2c) under SHC. The difference appears in (3b) in which the impact of a DC-line h on the flow on AC-line l is explicitly added[3]. The flow on an AC-line l as a result of a flow on a DC-line h is calculated with the nodal PTDFs $nPTDF_l^{n(h-)}$ and $nPTDF_l^{n(-h)}$ with $n(h-)$ and $n(-h)$ the starting/ending end of DC-line h. $I^{ACDC}_{n(h-),h}$ and $I^{ACDC}_{n(-h),h}$ equal 1 (or -1) if the flow on DC-line h is defined as flowing into (or away from) node $n(h-)$ or $n(-h)$ respectively, and is zero otherwise. Note that, because only cross-border DC-lines are monitored in the market, the impact of only cross-border DC-lines $h \in \mathcal{H}' \subset \mathcal{H}$ on AC-line l is captured.

B. Congestion management

Objective (4a) and Constraints (4b) to (4i) present the redispatch problem. We assume cost-based redispatch as instrument for congestion management. The decision variables in the day-ahead market clearing appear as a parameter. The decision variables in this problem are (i) the upward or downward adjustment of the scheduled output u_g and d_g of each non-intermittent generator g, (ii) a change of the curtailment of renewable energy sources Δc_n at each node n, and (iii) a change of the DC-flow Δf_h^{DC} on each DC-line h.

$$\min_{u_g, d_g, \Delta c_n, \Delta f_h^{DC}} \quad RDC = \sum_{g \in \mathcal{G}} Q_g^s \cdot MC_g \Big[u_g - d_g \Big] \tag{4a}$$

subject to

$$\sum_{g \in \mathcal{G}} u_g \cdot Q_g^s = \sum_{g \in \mathcal{G}} d_g \cdot Q_g^s \tag{4b}$$

$$\begin{aligned} -\bar{F}_l \leqslant \sum_{n \in \mathcal{N}} nPTDF_l^n \cdot \Big[\sum_{g \in \mathcal{G}(\mathcal{N})} & Q_g^s \cdot [v_g \\ +u_g - d_g] + R_n - c_n - \Delta c_n - Q_n^d \\ - \sum_{h \in \mathcal{H}} [f_h^{DC} + \Delta f_h^{DC}] \cdot I_{h,n} \Big] & \leqslant \bar{F}_l, \forall l \in \mathcal{L} \end{aligned} \tag{4c}$$

$$-\bar{F}_h^{DC} \leqslant f_h^{DC} + \Delta f_h^{DC} \leqslant \bar{F}_h^{DC}, \forall h \in \mathcal{H} \tag{4d}$$

$$0 \leqslant u_g \leqslant 1 - v_g, \forall g \in \mathcal{G} \tag{4e}$$

$$0 \leqslant d_g \leqslant v_g, \forall g \in \mathcal{G} \tag{4f}$$

$$-c_n \leqslant \Delta c_n \leqslant R_n - c_n, \forall n \in \mathcal{N} \tag{4g}$$

$$-f_h^{DC} \leqslant \Delta f_h^{DC} \leqslant \bar{F}_h^{DC} - f_h^{DC}, \forall h \in \mathcal{H} \tag{4h}$$

$$\sum_{h \in \mathcal{H}} f_h^{DC} \cdot I_{h,n} = R_n - c_n, \forall n \in \mathcal{N}' \tag{4i}$$

Constraint (4b) imposes that the power balance is kept. Constraint (4c) limits the flow on each AC-line l using the nodal PTDFs $nPTDF_l^n$ that also include the injection of the DC-lines h in the AC-grid. Constraint (4c) limits the flow on each DC-line h. Constraints (4e) to (4h) pose technical limits to the decision variables. Finally, Constraint (4i) describes a nodal power balance at the off-shore nodes $n \in \mathcal{N}' \subset \mathcal{N}$, i.e., the nodes that do not connect with an AC-line.

[3]This could also be explained with a virtual bidding zone at the end of a DC-line h if that end marks the connection between the DC-grid and AC-grid. The virtual bidding zone exports/imports to/from the AC-grid a quantity f_h^{DC}

III. Case Study

A. Data

We apply our models on a fictive power system, based on [10] and presented by Fig. 2. It consists of four zones on the mainland of which Table I presents total generation capacity by non-intermittent generators and renewable energy sources as well as total constant demand in the zone. There are six off-shore wind farms, each with a capacity of 500 MW, which are connected with DC-lines (yellow lines) both internally as with the mainland. Under the Off-shore Bidding Zone (OBZ) configuration, the off-shore nodes constitute a separate zone (visualised in Appendix A), while they are connected to a mainland zone under the Home Market (HM) configuration.

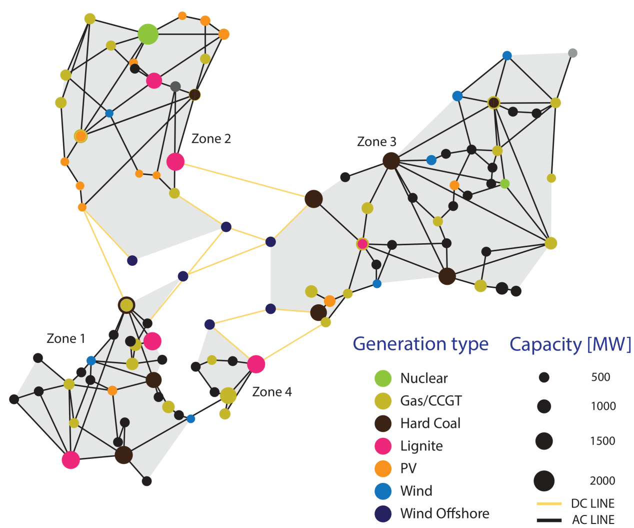

Fig. 2: Home Market (HM) configuration with generation capacity and load. The six off-shore nodes form a separate zone under the Off-shore Bidding Zone (OBZ) configuration.

TABLE I: Generation capacity of conventional power plants and renewable energy sources as well as total demand per zone, excluding the 6 off-shore nodes.

	Zone 1	Zone 2	Zone 3	Zone 4
Conv. generation cap. [MW]	11,837	11,410	12,220	3,000
RES generation cap. [MW]	1,115	3,391	2,657	0
Demand [MWh/h]	5,237	2,206	3,955	1,296

The flow-based parameters (RAMs and zonal PTDFs) appear as a parameter in the zonal market clearing algorithm. We assume the outcome of a nodal market clearing as the base case, and weight the GSKs pro rata with the generation capacity. Subsequently, the flow-based parameters can be calculated following [11]. Finally, we apply a MinRAM criterium of 70% on all AC-lines. This means that the commercial transmission capacity available in the day-ahead market in both directions (RAM_l^- and RAM_l^+, $\forall l \in \mathcal{L}$) is at least 70% of the physical transmission capacity, in line with EU regulations [12].

We assume the load factors of renewable energy sources on the mainland to be constant over all time steps at 0.2 for PV and 0.4 for on-shore wind for the sake of simplicity. The load factors of the off-shore wind farms vary over 160 time steps. We split up the off-shore region in the three most western off-shore nodes on the one hand and the three most eastern off-shore nodes on the other hand. Fig. 3 present the load factors for both the western and eastern off-shore region. The DC-lines and AC-lines have an average capacity of 646 MW and 504 MW respectively. We refer the reader to [10] for an exhaustive network description.

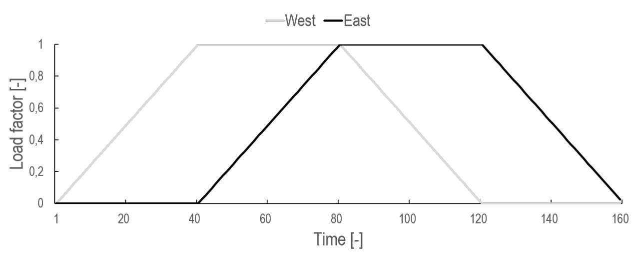

Fig. 3: Load factors for the three most Western off-shore nodes and the three most Eastern off-shore nodes.

B. Results

Fig. 4 presents the prices for off-shore wind farms under the HM and OBZ configuration while distinguishing between SHC and AHC, and with a nodal market as benchmark. The boxes show the quantiles while the dashed line shows the average. The kernel density is additionally plotted to visualise the distribution.

We make three observations. Firstly, the average price for the off-shore wind farms under the OBZ configuration is lower than under the HM configuration regardless of whether the grid is represented with SHC or AHC. The average prices under the OBZ configuration amount to 11.55 €/MWh and 8.45 €/MWh for the two market designs, while under the HM configuration, the average prices are 35.08 €/MWh, 35.01 €/MWh. The price from a nodal market, optimally reflecting generation and transmission constraints in price formation, lays in between the OBZ and HM configuration with 15.28 €/MWh on average. Prices are generally lower under the OBZ configuration because congestion between an off-shore wind farm and one or more nodes on the mainland limits trade between these zones, hence, resulting in a price difference between the off-shore wind farm and the mainland zone, which is not the case under the HM configuration. Put differently, the market signals the congestion through a price difference under the OBZ configuration.

Secondly, the variation of prices is higher under the OBZ configuration compared to the HM configuration. The difference between the maximum and minimum price for off-shore wind farms under the HM configuration (SHC and AHC) is 5.28 €/MWh, while it amounts to 34 €/MWh (SHC) and 47.42 €/MWh (AHC) under the OBZ configuration. This is a consequence of valuing wind energy at 0 €/MWh during periods of congestion in the OBZ.

Thirdly, there exists only little difference in prices for off-shore wind farms between SHC and AHC under the HM configuration, while prices are lower using AHC compared to SHC under the OBZ configuration. Specifically, while the difference between the average price of SHC and AHC under the HM configuration is 0.07 €/MWh, the difference is 3.1 €/MWh under the OBZ configuration. This is because the OBZ configuration comes with more DC-lines that are both inter-zonal lines and connecting with the AC-grid. Subsequently, the ability of AHC to capture the impact of the DC-lines on the AC-grid more accurately (cfr. constraint (3b) compared to constraint (2b)) leads to detection of congestion (full utilization of commercially available transmission capacity), hence, 0 €/MWh in the off-shore zone.

TABLE II: Results of the case study under the HM and OBZ configuration with a nodal market as benchmark. We distinguish between SHC and AHC.

		OBZ	HM
Nodal	Revenues [M€]	3.637	
	Curtailment [GWh]	0	
	Wind at zero-price [GWh]	89.988	
	Wind at price >0 [GWh]	150.012	
	Congestion rent [M€]	9.594	
	Day-ahead cost [M€]	39.288	
	Redispatch cost [€]	0	
Zonal w/ SHC	Revenues [M€]	3.394	8.239
	Curtailment [GWh]	0	0
	Wind at zero-price [GWh]	131.888	0
	Wind at price >0 [GWh]	108.112	240.0
	Congestion rent [M€]	12.948	1.245
	Day-ahead cost [M€]	37.001	35.791
	Redispatch cost [M€]	8.920	10.129
Zonal w/ AHC	Revenues [M€]	0.947	8.193
	Curtailment [GWh]	18.522	0
	Wind at zero-price [GWh]	190.728	0
	Wind at price >0 [GWh]	30.750	240.0
	Congestion rent [M€]	2.371	1.287
	Day-ahead cost [M€]	40.137	35.742
	Redispatch cost [M€]	5.784	10.178

Table II shows revenues and curtailment volumes of the off-shore wind farms, sold off-shore wind volumes in the market at a price equal to or higher than zero, congestion rents as well as day-ahead generation and redispatch costs.

Firstly, revenues for off-shore wind farms decrease under the OBZ configuration compared to the HM configuration regardless of the representation of the grid in the market. This is mainly driven by a decreased average price (see Fig. 4) as curtailment is zero except under the OBZ configuration in combination with AHC. Specifically, a share of 55% (131.888 GWh) and 79% (190.728 GWh) of the total off-shore wind power availability (240 GWh) is sold at a price of 0 €/MWh under SHC and AHC. Contrary, under the HM configuration, the share of off-shore wind power sold at 0 €/MWh amounts to 0% for the two grid representations.

Secondly, the congestion rent increases under the OBZ

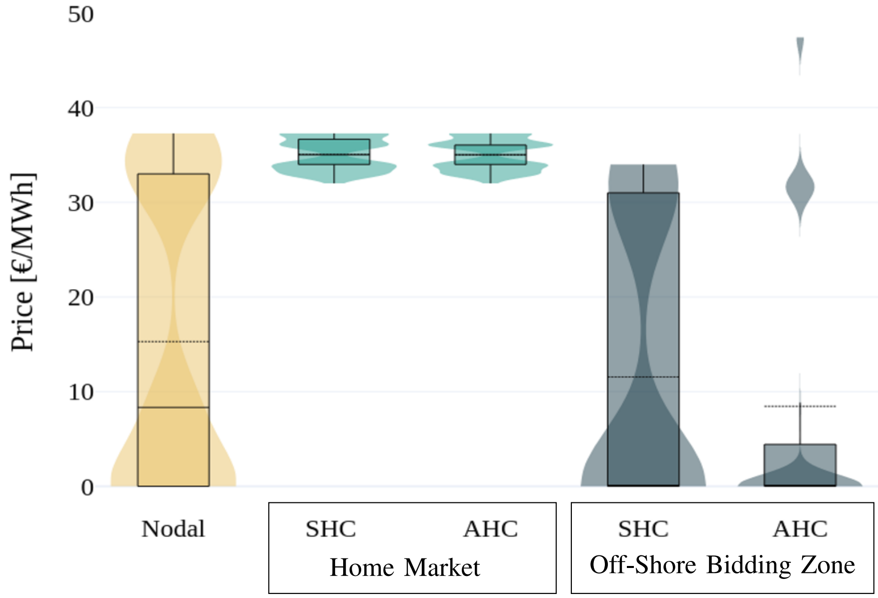

Fig. 4: Prices for off-shore wind farms under the HM and OBZ configuration with a nodal market as benchmark. We distinguish between SHC and AHC. The boxes show the 25th and 75th quantiles and the median while the dashed line shows the average. The kernel density visualises the distribution. Prices under the HM configuration are on average higher than under a nodal market, while prices under the OBZ configuration are on average lower.

configuration compared to the HM configuration. This is a consequence of an increased amount of cross-border lines on which a price difference exists.

Thirdly, day-ahead generation costs are higher under the OBZ configuration compared to the HM configuration because the grid constraints are more restrictive in the market clearing algorithm: the DC-line that connects an off-shore wind farm with the mainland is not monitored under the HM configuration as it is not a cross-border line. However, this increase in day-ahead generation costs is offset by a decrease in redispatch costs in our case study. Specifically, the sum of the day-ahead generation cost and redispatch cost in both the OBZ and HM configuration is constant and equal to 45.920 M€ for all two grid representations[4]. In real-time, after redispatch, these six cases lead to an identical grid operation. Nevertheless, the share of the total costs that are market-based (day-ahead generation cost) or made by TSOs (redispatch cost) differs. The OBZ configuration outperforms the HM configuration in capturing and signaling generation and transmission scarcity, and therefore leads to decreased costs for congestion management. Looking at the grid representations in the market specifically, AHC outperforms SHC as the market captures the expected flows more accurately, in our case study leading to a more restrictive market clearing and, hence, higher day-ahead generation costs and lower redispatch costs.

IV. Policy implications & Conclusion

This paper shows that a separate bidding zone for off-shore wind farms leads to a transfer of welfare: the producers' surplus of off-shore wind farm owners decreases and the congestion rent for TSOs increases. Firstly, prices for off-shore wind farms drop on average and vary more. A price of 0 €/MWh occurs when commercial transmission capacities with mainland are fully used. As such, the frequency of prices of 0 €/MWh depends on the dimensions[5] of the transmission grid. Secondly, the congestion rent increases because additional price differences over the grid elements emerge under an OBZ configuration compared to a HM configuration. However, it is important to note that an OBZ configuration comes with an increase in day-ahead generation costs because of a more accurate consideration of the grid constraints in the market clearing algorithm. The increase in day-ahead generation costs is offset by an equal decrease in redispatch costs. However, redispatch actions are more complex in reality.

Lower revenues from day-ahead markets for off-shore wind farm owners under an OBZ configuration has important implications for investments in generation capacity and, hence, long-term renewable energy targets. Support instruments for off-shore wind farms should be carefully re-assessed.

Future work should focus on different topologies and dimensions of power networks as it impacts the magnitude of the revealed effects.

References

[1] European Commission, "Communication from the commission to the European parliament, the council, the European economic and social committee and the committee of the regions," 2020,

[4]Note that this depends on how the redispatch model is formulated. Our paper considers cost-based redispatch without transaction costs.

[5]This paper applies arbitrarily determined transmission line capacities to explicitly show the effect where prices of 0 €/MWh for off-shore wind farms occur.

https://eur-lex.europa.eu/legal-content/EN/TXT/PDF/?uri=CELEX:52020DC0741&from=EN, accessed on 03.02.2022.

[2] North Sea Wind Power Hub, "Towards the first hub-and-spoke project," 2021, https://northseawindpowerhub.eu/sites/northseawindpowerhub.eu/files/media/document/NSWPH_Concept\%20Paper_05_2021_v2.pdf, accessed on 03.02.2022.

[3] NorthConnect, "NorthConnect," 2021, https://northconnect.co.uk/, accessed on 03.02.2022.

[4] THEMA Consulting Group, "Market Arrangements for Offshore Hybrid Projects in the North Sea," 2020, https://op.europa.eu/en/publication-detail/-/publication/28ff740c-25aa-11eb-9d7e-01aa75ed71a1/language-en, accessed on 24.02.2022.

[5] European Commission, "Communication from the commission to the European Parliament, the Council, the European Econonmic and Social Committee and the Committee of the Regions: An EU Strategy to harness the potential of offshore renewable energy for a climate neutral future." 2020, https://ec.europa.eu/energy/sites/ener/files/offshore_renewable_energy_strategy.pdf, accessed on 24.02.2022.

[6] PROMOTioN - Progress on Meshed HVDC Offshore Transmission Networks, "D12.4 Deployment plan for future European offshore grid," 2020, https://www.promotion-offshore.net/fileadmin/PDFs/D12.4_-_Final_Deployment_Plan.pdf, accessed on 24.02.2022.

[7] The North Seas Countries' Offshore Grid Initiative, "Discussion Paper 2: Integrated Offshore Networks and The Electricity Target Model. Deliverable 3." 2014, https://www.benelux.int/files/4514/0923/4100/Market_Arrangements_Paper_Final_Version_28_July_2014.pdf, accessed on 24.02.2022.

[8] ENTSO-E, "Position Paper on Offshore Development: Assessing Selected Financial Support Options for Renewable Generation," 2021, https://eepublicdownloads.azureedge.net/clean-documents/Publications/Position\%20papers\%20and\%20reports/entso-e_pp_Offshore_Development_05_Financial_Support_211102.pdfl, accessed on 24.02.2022.

[9] C. Müller, A. Hoffrichter, H. B. Büchel, A. Schwarz, and A. Schnettler, "Integration of hvdc-links into flow-based market coupling: Standard hybrid market coupling versus advanced hybrid market coupling," in *CIGRE Symposium*, 2017.

[10] D. Schönheit, M. Kenis, L. Lorenz, D. Möst, E. Delarue, and K. Bruninx, "Toward a fundamental understanding of flow-based market coupling for cross-border electricity trading," *Advances in Applied Energy*, vol. 2, p. 100027, 2021. [Online]. Available: https://www.sciencedirect.com/science/misc/pii/S2666792421000202

[11] K. Van den Bergh, J. Boury, and E. Delarue, "The Flow-Based Market Coupling in Central Western Europe: Concepts and Definitions," *The Electricity Journal*, vol. 29, no. 1, pp. 24–29, 2016.

[12] Council of the European Union and European Parliament, "Regulation (EU) 2019/943 of the European Parliament and of the Council of 5 June 2019 on the internal market for electricity," pp. 54–124, 2019, accessed on 13.04.2022. [Online]. Available: http://data.europa.eu/eli/reg/2019/943/oj

Appendix
Off-shore Bidding Zone configuration

Figure 5 visualises the OBZ configuration. The DC-lines that connect with AC-lines are cross-border lines as opposed to under the HM configuration. Hence, the flow on these lines is a decision variable, capped by the NTC, in the market clearing algorithm. As a result, the impact of the flow on these DC-lines on the flow on the AC-lines can be captured under AHC, which is not the case under the HM configuration.

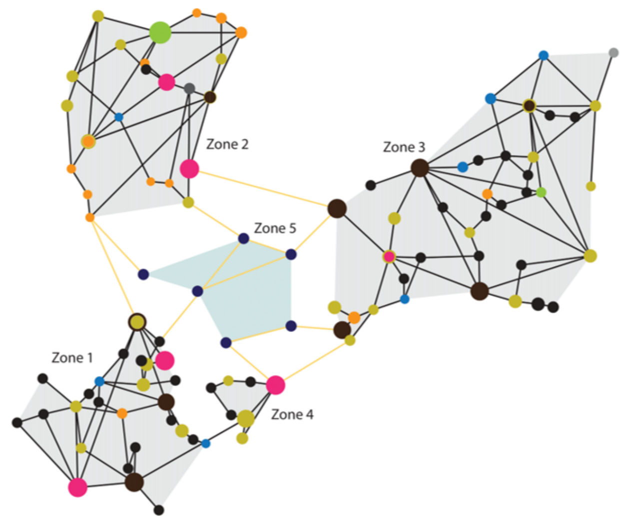

Fig. 5: Off-shore Bidding Zone (OBZ) configuration with generation capacity and load. The six off-shore nodes form a separate zone.